**9214** *Inorg. Chem.* **2009**, *48*, 9214–9221
DOI: 10.1021/ic9010218

Inorganic Chemistry
Article

# Ligand Reactivity in Diarylamido/Bis(Phosphine) PNP Complexes of $Mn(CO)_3$ and $Re(CO)_3$

**Alexander T. Radosevich,[†] Jonathan G. Melnick,[†] Sebastian A. Stoian,[†] Deborha Bacciu,[‡] Chun-Hsing Chen,[‡] Bruce M. Foxman,[‡] Oleg V. Ozerov,*[,‡,§] and Daniel G. Nocera*[,†]**

[†]*Department of Chemistry, Massachusetts Institute of Technology, Cambridge, Massachusetts 02139,*
[‡]*Department of Chemistry, Brandeis University, 415 South Street, Waltham, Massachusetts 02454, and*
[§]*Department of Chemistry, Texas A&M University, College Station, Texas 77842*

Received May 26, 2009

The syntheses of meridionally ligated tricarbonyl complexes (PNP)$Mn(CO)_3$ and (PNP)$Re(CO)_3$ are described (PNP= [2-P($CHMe_2$)$_2$-4-$MeC_6H_3$]$_2$$N^-$). Cyclic voltammograms show reversible one-electron redox couples for both parent compounds (−0.34 V vs $Cp_2Fe^{0/+}$ for (PNP)$Mn(CO)_3$, −0.25 V vs $Cp_2Fe^{0/+}$ for (PNP)$Re(CO)_3$), and chemical oxidation with AgOTf results in formation of the corresponding paramagnetic triflate salts [(PNP)$Mn(CO)_3$]OTf and [(PNP)$Re(CO)_3$]OTf. Electron paramagnetic resonance spectra and computational results indicate that this event is primarily ligand centered; allylation of the organic ligand moiety of [(PNP)$Mn(CO)_3$]OTf with allyltributylstannane is consistent with this assignment. The oxidation (PNP)$Mn(CO)_3$ to [(PNP)$Mn(CO)_3$]OTf results in a shift in average CO stretching frequency of 30 $cm^{-1}$; protonation of (PNP)$Mn(CO)_3$ with TfOH to form [(PNHP)$Mn(CO)_3$]OTf results in a similar magnitude shift.

## Introduction

Appreciation for the interplay between transition metals and redox non-innocent ligands, a factor long-recognized in coordination[1] and bioinorganic chemistry,[2] is burgeoning in chemically reacting systems.[3] Working in concert with redox active metals, non-innocent ligands have been shown to engender unexpected bond activation processes through dynamic modulation of metal electron density.[4,5] Alternatively, in conjunction with non-redox active metals (e.g., metals with $d^0$ electron count or unfavorable redox potentials), non-innocent ligands support reactivity that would be otherwise unavailable to metals in these electronic configurations.[6−8] Additionally, exploiting valence isomerism in redox active ligands, for example, in conjunction with storage of electron−hole equivalents in energy conversion schemes, has been investigated.[9−13]

The diarylamido-based PNP-pincer ligands (e.g., **1**) have been demonstrated to support a rich array of transition metal chemistry.[14−24] While the structural implications of the rigid ligand scaffold have been noted, the PNP moiety has been considered largely to be a static electronic spectator to the metal-center redox chemistry. Several studies though have recently suggested the redox non-innocence of **1** in complexes

*To whom correspondence should be addressed. E-mail: ozerov@mail.chem.tamu.edu (O.V.O.), nocera@mit.edu (D.G.N.).

(1) Holm, R. H.; Balch, A. L.; Davison, A.; Maki, A. H.; Berry, T. E. *J. Am. Chem. Soc.* **1967**, *89*, 2866.
(2) Sono, M.; Roach, M. P.; Coulter, E. D.; Dawson, J. H. *Chem. Rev.* **1996**, *96*, 2841.
(3) Chaudari, P.; Wieghardt, K. *Prog. Inorg. Chem.* **2001**, *50*, 151.
(4) Bart, S. C.; Chlopek, K.; Bill, E.; Bouwkamp, M. W.; Lobkovsky, E.; Neese, F.; Wieghardt, K.; Chirik, P. J. *J. Am. Chem. Soc.* **2006**, *128*, 13901.
(5) Pierpont, C. G. *Coord. Chem. Rev.* **2001**, *216*, 99.
(6) Blackmore, K. J.; Ziller, J. W.; Heyduk, A. F. *Inorg. Chem.* **2005**, *44*, 5559.
(7) Haneline, M. R.; Heyduk, A. F. *J. Am. Chem. Soc.* **2006**, *128*, 8410.
(8) Zarkesh, R. A.; Ziller, J. W.; Heyduk, A. F. *Angew. Chem., Int. Ed.* **2008**, *47*, 4715.
(9) Bachmann, J.; Nocera, D. G. *J. Am. Chem. Soc.* **2004**, *126*, 2829.
(10) Bachmann, J.; Nocera, D. G. *J. Am. Chem. Soc.* **2005**, *127*, 4730.
(11) Bachmann, J.; Nocera, D. G. *Inorg. Chem.* **2005**, *44*, 6930.
(12) Bachmann, J.; Hodgkiss, J. M.; Young, E. R.; Nocera, D. G. *Inorg. Chem.* **2007**, *46*, 607.
(13) Bachmann, J.; Teets, T. A.; Nocera, D. G. *Dalton Trans.* **2008**, 4549.
(14) van der Boom, M. E.; Milstein, D. *Chem. Rev.* **2003**, *103*, 1759.
(15) Ozerov, O. V. In *The Chemistry of Pincer Compounds*; Morales-Morales, D., Jensen, C., Eds.; Elsevier: Amsterdam, 2007; p 287.
(16) Ozerov, O. V.; Guo, C.; Papkov, V. A.; Foxman, B. M. *J. Am. Chem. Soc.* **2004**, *126*, 4792.
(17) Bailey, B. C.; Fan, H.; Baum, E. W.; Huffman, J. C.; Baik, M.-H.; Mindiola, D. J. *J. Am. Chem. Soc.* **2005**, *127*, 16016.
(18) Gatard, S.; Chen, C.-H.; Foxman, B. M.; Ozerov, O. V. *Organometallics* **2008**, *27*, 6257.
(19) Kilgore, U. J.; Sengelaub, C. A.; Fan, H.; Tomaszewski, J.; Karty, J. A.; Baik, M.-H.; Mindiola, D. J. *Organometallics* **2009**, *28*, 843.
(20) Whited, M. T.; Grubbs, R. H. *J. Am. Chem. Soc.* **2008**, *130*, 5874.
(21) Calimano, E.; Tilley, T. D. *J. Am. Chem. Soc.* **2008**, *130*, 9226.
(22) Harkins, S. B.; Mankad, N. P.; Miller, A. J. M.; Szilagyi, R. K.; Peters, J. C. *J. Am. Chem. Soc.* **2008**, *130*, 3478.
(23) Liang, L. C.; Lin, J. M.; Hung, C. H. *Organometallics* **2003**, *22*, 3007.
(24) Winter, A. M.; Eichele, K.; Mack, H. G.; Potuznik, S.; Mayer, H. A.; Kaska, W. C. *J. Organomet. Chem.* **2003**, *682*, 149.


Published on Web 09/08/2009

**Scheme 1.** Synthesis of (PNP)M(CO)$_3$ and Related Compounds

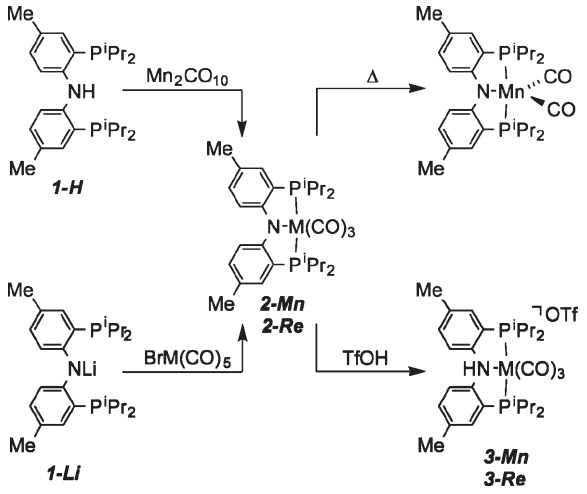


of nickel(II)[25] and copper(I).[22,26] These findings, together with the facile oxidation of related free anilines and diarylamines to the corresponding anilinyl radical cations,[27] implicate a more integral function for **1** in modulating the reactivity of bound metal centers during the course of redox bond activation processes.

In the interest of better understanding the ligand parameters that influence the metal-based reactivity in PNP pincer complexes, we describe here the incorporation of $Mn(CO)_3^+$ and $Re(CO)_3^+$ fragments into the PNP coordination environment. By doing so, we interrogate the effect of ligand protonation and oxidation state on the electronic structure of the $M(CO)_3$ unit employing the useful infrared spectroscopic handle. Our results are consistent with the presence of accessible ligand centered oxidation events in these complexes, which we further demonstrate by reaction of the resulting ligand radical cations with trapping agents.

## Results

**Synthesis and Protonation of (PNP)M(CO)$_3$ Complexes.** The PNP-pincer ligated manganese compound **2-Mn** was prepared by two methods. Reaction of lithium amide **1-Li** with $BrMn(CO)_5$ in refluxing dioxane resulted in the formation of **2-Mn** as an orange diamagnetic solid (Scheme 1). Alternatively, **2-Mn** could be formed by heating a solution of **1-H** in hexamethyldisiloxane with $Mn_2(CO)_{10}$. NMR spectra (see Experimental Section for details) of **2-Mn** produced in these ways show proton resonances consistent with the desired $C_{2v}$-symmetric coordination mode; a singlet in the $^{31}P\{^1H\}$ NMR spectrum at 84.1 ppm is consistent with the symmetry equivalence of the phosphines. The solid state structures confirm the tridentate coordination of the PNP ligand (Figure 1), an overall pseudooctahedral geometry of the complexes, and a *mer* orientation of the carbonyl ligands (Figure 1). The pincer ligand is bound to the metal with a Mn−N distance of 2.076(2) Å, Mn−P distances of 2.280(1) Å, and a P−Mn−P angle of 158.6(1)° (Table 1). The three C≡O stretching frequencies for the *mer* carbonyl ligands resonate at 2020, 1917, and 1896 cm$^{-1}$.

Treatment of $BrRe(CO)_5$ with lithium amide **1-Li** in refluxing dioxane resulted in isolation of the rhenium congener **2-Re** as a yellow diamagnetic compound in 41% yield.[28] The $^{31}P\{^1H\}$ NMR resonance for **2-Re** was found as a sharp singlet at 45.4 ppm. The pseudooctahedral geometry of this complex is evident in the solid state structure where the metal coordination environment is defined by a Re−N distance of 2.191(4) Å, Re−P distances of 2.398(1) Å, and a *mer* arrangement of the carbonyl ligands ($\nu_{CO}$ = 2026, 1909, 1891 cm$^{-1}$).

Refluxing a solution of **2-Mn** in mesitylene for 6 h results in partial conversion (ca. 40%) to $(PNP)Mn(CO)_2$ as judged by $^1H$ NMR spectroscopy. Unfortunately, $(PNP)Mn(CO)_2$ is not thermally stable for prolonged periods at elevated temperatures and, as a result, further heating of the mesitylene solution resulted in decomposition of $(PNP)Mn(CO)_2$. Increased conversion of **2-Mn** to $(PNP)Mn(CO)_2$ was obtained with milder conditions; heating of **2-Mn** in fluorobenzene solution at 60 °C in the presence of the carbonylophilic complex $[(p\text{-cymene})RuCl_2]_2$ resulted in about 70% conversion of **2-Mn** to $(PNP)Mn(CO)_2$. The $^{31}P\{^1H\}$ NMR resonance of $(PNP)Mn(CO)_2$ shifts only slightly upfield to 83.0 ppm, but the carbonyl stretches ($\nu_{CO}$ = 1900, 1838 cm$^{-1}$) are indicative of an increased backbonding effect relative to the tricarbonyl complex **2-Mn**. Structural parameters for $(PNP)Mn(CO)_2$ obtained from a sample that co-crystallized with **2-Mn** indicate that $(PNP)Mn(CO)_2$ adopts a Y-shape five-coordinate structure with the carbonyls and the pincer amide forming the Y. The C−Mn−C angle of about 90° is also consistent with the near-equal intensities of the symmetric and the antisymmetric $\nu_{CO}$ bands in the solution IR spectrum.[29] Structural preferences of five-coordinate d$^6$ complexes have been discussed elsewhere.[30−32] Despite repeated attempts, **2-Re** could not be decarbonylated by either thermolytic or photolytic methods.

Treatment of **2-Mn** and **2-Re** with trifluoromethanesulfonic acid resulted in stoichiometric protonation of the ligand's nitrogen atom. This protonation event decreases the symmetry of **2-Mn** and **2-Re** from $C_{2v}$ to $C_s$, as is evident in the $^1H$ NMR spectra of the product compounds **3-Mn** and **3-Re**. Specifically, the previously equivalent isopropyl moieties on the phosphines are split into two inequivalent sets (*syn* and *anti* with respect to the N−H proton) as can be identified by the two resonances at 2.95 and 2.36 ppm for the Mn-PC*H*Me$_2$ proton in **3-Mn** and at 2.53 and 2.16 ppm for the Re-PC*H*Me$_2$ in **3-Re**. The presence of a single phosphorus resonance in the $^{31}P\{^1H\}$ NMR spectra for **3-Mn** (78.2 ppm) and **3-Re** (42.1 ppm) is indicative of **3-Mn** and **3-Re** possessing $C_s$-symmetry in solution, although the data are insufficient

(25) Adhikari, D.; Mossin, S.; Basuli, F.; Huffman, J. C.; Szilagyi, R. K.; Meyer, K.; Mindiola, D. J. *J. Am. Chem. Soc.* **2008**, *130*, 3676.
(26) Harkins, S. B.; Peters, J. C. *J. Am. Chem. Soc.* **2005**, *127*, 2030.
(27) Merenyi, G.; Lind, J. In *N-Centered Radicals*; Alfassi, Z. B., Ed.; Wiley-VCH: Weinheim, Germany, 1998; p 599.
(28) For related monoanionic PNP complexes of rhenium, see: Ozerov, O. V.; Watson, L. A.; Pink, M.; Caulton, K. G. *J. Am. Chem. Soc.* **2007**, *129*, 6003.
(29) Cotton, F. A.; Wilkinson, G. *Advanced Inorganic Chemistry*; John Wiley: New York, 1988; p 1035.
(30) Lam, W. H.; Shimada, S.; Batsanov, A. S.; Lin, Z.; Marder, T. B.; Cowan, J. A.; Howard, J. A. K.; Mason, S. A.; McIntyre, G. J. *Organometallics* **2003**, *22*, 4557.
(31) Rachidi, I. E.-I.; Eisenstein, O.; Jean, Y. *New J. Chem.* **1990**, *14*, 671.
(32) Olivan, M.; Eisenstein, O.; Caulton, K. G. *Organometallics* **1997**, *16*, 2227.

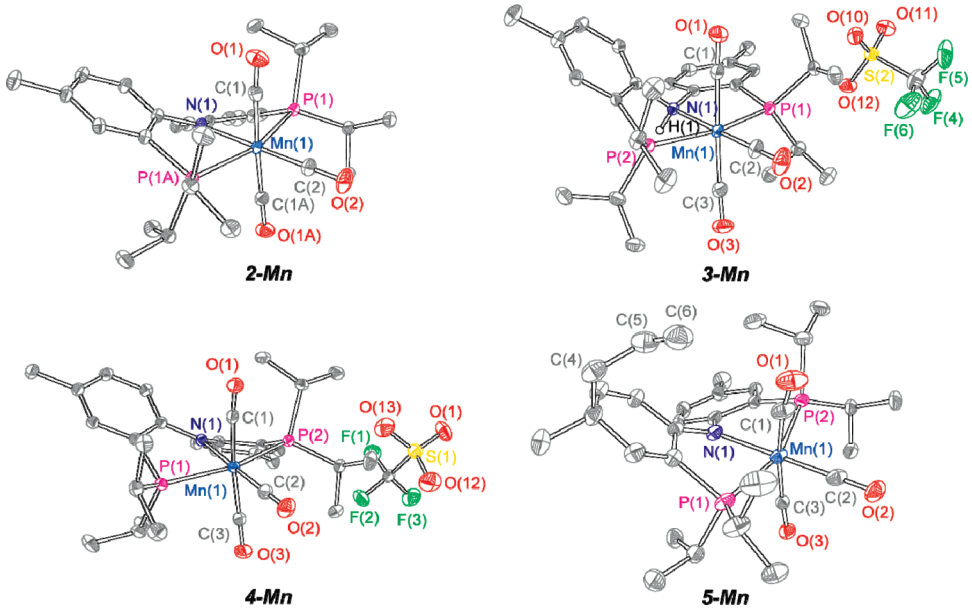


**Figure 1.** Ellipsoid plots of compounds **2-Mn**, **3-Mn**, **4-Mn**, and **5-Mn**. Hydrogen atoms and noncoordinating solvent molecules are omitted for clarity. For **3-Mn**, one of two crystallographically independent molecules is depicted. For **5-Mn**, a noncoordinating counterion is omitted. Data collected at 100 K with thermal ellipsoids drawn at 50% probability.

**Table 1.** Selected Bond Lengths and Angles for Solid State Structures **2**−**4**

| metric | 2-Mn | 3-Mn | 4-Mn | 2-Re | 3-Re | 4-Re |
|---|---|---|---|---|---|---|
| M−C(1) | 1.838(1) | 1.844(3) | 1.850(2) | 1.972(5) | 1.996(5) | 1.986(6) |
| M−C(2) | 1.784(2) | 1.777(3) | 1.815(2) | 1.930(6) | 1.900(5) | 1.934(6) |
| M−N | 2.076(2) | 2.159(2) | 2.029(2) | 2.191(4) | 2.251(4) | 2.155(5) |
| M−P(1) | 2.280(3) | 2.286(1) | 2.305(1) | 2.398(1) | 2.408(1) | 2.412(2) |
| C(1) −O(1) | 1.145(2) | 1.141(3) | 1.142(3) | 1.149(6) | 1.142(6) | 1.145(7) |
| C(2) −O(2) | 1.158(2) | 1.153(3) | 1.148(3) | 1.153(8) | 1.170(5) | 1.156(7) |
| C(1) −M−C(2) | 88.2(1) | 89.5(1) | 85.0(1) | 86.3(1) | 86.9(2) | 85.0(2) |
| C(1) −M−C(3) | 176.3(1) | 175.4(1) | 170.8(1) | 172.5(2) | 173.4(2) | 170.7(2) |

to distinguish between possible $\kappa^3$-*P,N,P* and $\kappa^2$-*P,P* binding modes consistent with this symmetry restriction.

Examining the structural parameters determined for a single-crystal of **3-Mn** by X-ray diffraction (Figure 1), we find that protonation of the ligand nitrogen results in a lengthening of the Mn−N bond relative to **2-Mn** by 0.083 Å to 2.159(1) Å. Carbonyl stretches in **3-Mn** shift 26 $cm^{-1}$ in aggregate toward higher wavenumbers ($\nu_{CO}$ = 2039, 1949, 1923 $cm^{-1}$) with respect to **2-Mn** as a result of this protonation event. A similar trend is evident in the case of **3-Re**. Protonation of the ligand nitrogen atom results in lengthening of the Re−N distance by 0.06 Å to 2.251(1) Å, and a $\Delta\nu = 31$ $cm^{-1}$ average shift for the carbonyl frequencies ($\nu_{CO}$ = 2049, 1943, 1928 $cm^{-1}$).[33,34] This effect likely arises from two factors: the protonation event causes the pyramidalization of the N atom thus diminishing the interaction of the p$\pi$ lone electron pair with a d$\pi$ metal orbital, and the overall charge of the complex reduces the proclivity for metal backbonding to the carbonyls.

**Electrochemistry of (PNP)M(CO)$_3$ Complexes.** A cyclic voltammogram of **2-Mn** in acetonitrile (0.1 M $n$Bu$_4$NPF$_6$, $T$ = 293 K, scan rate = 100 mV/s, platinum working electrode) shows a chemically reversible wave at −0.34 V versus $Cp_2Fe^{o/+}$. Cyclic voltammetry of **2-Re** under identical conditions indicates the presence of a single reversible redox process centered at −0.25 V versus $Cp_2Fe^{o/+}$ (Table 2). The potentials at which this redox process occurs for both **2-Mn** and **2-Re** are conspicuously low for metal-centered oxidation of $d^6$ $Mn^I(CO)_3$ and $Re^I(CO)_3$ complexes. For instance, the anodic one-electron oxidation of $CpMn(CO)_3$ was found to occur at +0.92 V vs $Cp_2Fe^{o/+}$, and that for $Cp^*Mn(CO)_3$ was identified at +0.64 V vs $Cp_2Fe^{o/+}$.[35] These oxidation events, which were characterized as being significantly metal-based and result in formation of the corresponding Mn(II) 17e$^-$ paramagnetic complexes, are between 0.98 and 1.26 V more positive than that found for **2-Mn**. In a similar vein, the redox couples $CpRe(CO)_3^{0/+}$ and $Cp^*Re(CO)_3^{0/+}$ were identified at +1.16 V and +0.91 V vs $Cp_2Fe^{o/+}$, respectively.[36] Here, the metal centered oxidation for these compounds is found at a potential at least 1.16 V more positive than that for **2-Re**. Though not central to this study, a second oxidation event is evident for both **2-Mn** and **2-Re** in acetonitrile at higher potentials. For the manganese derivative, this process occurs at +0.81 V vs $Cp_2Fe^{o/+}$ and is quasi-reversible. The rhenium analogue displays an irreversible wave ($E_{pa}$ = +0.93) for the corresponding process. We have been unable to isolate the manganese compound associated with the oxidation wave at +0.81 V by either chemical ($NOBF_4$. $CH_2Cl_2$) or electrochemical means (controlled potential electrolysis, platinum mesh electrode, 0.1 M $n$-BuNPF$_6$, $T$ = 293 K, $CH_2Cl_2$), despite its apparent persistence on the electrochemical time scale.

**Chemical Oxidation of (PNP)M(CO)$_3$ Complexes.** Consistent with the electrochemistry, the one-electron

(33) Hevia, E.; Pérez, J.; Riera, V.; Miguel, D. *Organometallics* **2002**, *21*, 1966.
(34) Gabrielsson, A.; Busby, M.; Matousek, P.; Towrie, M.; Hevia, E.; Cuesta, L.; Perez, J.; Záliš, S.; Vlček, A. *Inorg. Chem.* **2006**, *45*, 9789.
(35) Laws, D. R.; Chong, D.; Nash, K.; Rheingold, A. L.; Geiger, W. E. *J. Am. Chem. Soc.* **2008**, *130*, 9859.
(36) Chong, D.; Nafady, A.; Costa, P. J.; Calhorda, M. J.; Geiger, W. E. *J. Am. Chem. Soc.* **2005**, *127*, 15676.

**Table 2.** Cyclic Voltammetry and Infrared Data for **2**−**4**

| compound | $E_{1/2}$ (V)[a] | $\nu_{CO}$/cm$^{-1}$[b] | $\nu_{CO}$ (avg)/cm$^{-1}$[c] |
|---|---|---|---|
| **2-Mn** | −0.34 | 2020, 1917, 1896 | 1944 |
| **3-Mn** | | 2039, 1949, 1923 | 1970 |
| **4-Mn** | 0.81 | 2032, 1951, 1938 | 1974 |
| **2-Re** | −0.25 | 2026, 1909, 1891 | 1942 |
| **3-Re** | | 2048, 1943, 1929 | 1973 |
| **4-Re** | 0.91[d] | 2054, 1951, 1934 | 1980 |

[a] $E_{1/2}$ vs $Cp_2Fe^{0/+}$, 0.1 M $TBAPF_6$ in MeCN, 100 mV/s, Pt disk. [b] KBr pellet. [c] $\nu_{CO} = [(\nu_s + \nu'_a + \nu''_a)/3]$. [d] $E_{pa}$ vs $Cp_2Fe^{0/+}$, 0.1 M $TBAPF_6$ in MeCN, 100 mV/s, Pt disk.

**Scheme 2.** Chemical Oxidation of $(PNP)M(CO)_3$

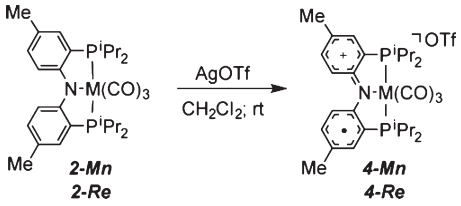


oxidized compounds **4-Mn** and **4-Re** could be prepared by treatment of **2-Mn** and **2-Re**, respectively, with silver(I) triflate (Scheme 2). X-ray crystallography of the blue paramagnetic products **4-Mn** (Figure 1) and **4-Re** revealed that the $Mn-C_{CO}$ and $Re-C_{CO}$ distances are only minimally affected by oxidation (Table 1). In the manganese case, the mutually trans-disposed carbonyls experience only a 0.012(2) Å perturbation (1.838(1) Å → 1.850(2) Å), while the carbonyl *trans* to N is affected by 0.031(3) Å (1.784(2) Å →1.815(2) Å). The effect of oxidation on the $Re-C_{CO}$ distances is even more subtle; neither apical nor basal carbonyls is affected by more than 0.015 Å following oxidation. Additionally, infrared spectra indicate that the average C≡O stretching frequency for the manganese series shifts only 30 cm$^{-1}$, from 1944 cm$^{-1}$ in **2-Mn** to 1974 cm$^{-1}$ in **4-Mn**, upon oxidation (Table 2). A similar magnitude change ($\Delta\nu = 38$ cm$^{-1}$) is observed in the oxidation of **2-Re** to **4-Re**. Metal-centered oxidation that significantly reduces the d-orbital occupancy and consequently the $\pi$-back-bonding effect has been shown to result in more marked lengthening of the metal−carbon bonds and larger differences in the C≡O stretching frequencies. In particular, Geiger has shown that the oxidation of the half-sandwich $CpMn(CO)_3$ to $[CpMn(CO)_3]^+$, an oxidation that has been shown to significantly engage Mn d-electrons, results in a 115 cm$^{-1}$ shift in average C≡O stretching frequency.[35] The oxidation of $CpRe(CO)_3$ to $[CpRe(CO)_3]^+$ similarly causes the carbonyl frequencies to shift about 100 cm$^{-1}$, consistent with a diminution of the formal d-electron count.[37] Congruent with this observation, the ligand centered oxidation of the metal catecholate complexes $[Mn^I(CO)_3(O_2C_6H_2{}^tBu_2)]^-$ and $[Re(CO)_3(thf)(O_2C_6H_2{}^tBu_2)]^-$ leads to a shift in $\nu_{CO}$ by 36 cm$^{-1}$ and 46 cm$^{-1}$, respectively.[38]

**Electron Paramagnetic Resonance (EPR) Spectroscopic and Computational Investigation of [(PNP)M(CO)$_3$]OTf Complexes.** The X-band EPR spectra of **4-Mn** and **4-Re** in $CH_2Cl_2$ solutions were recorded at room temperature in liquid phase as well as at cryogenic temperatures between 4.2 and 100 K for frozen samples. Both complexes exhibit signals that correspond to isolated Kramers doublets.

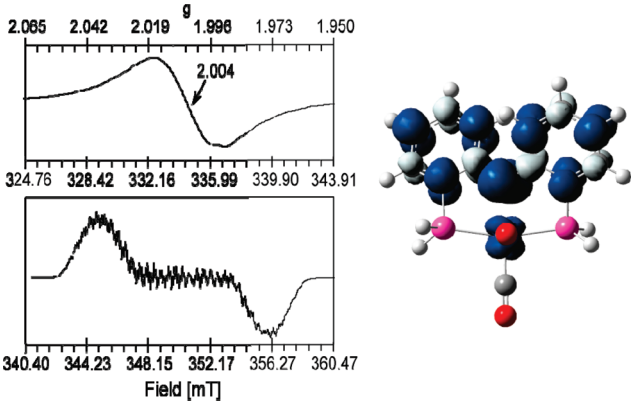


**Figure 2.** Left: EPR spectra of **4-Mn** at 4.2 K (top: 9.386 GHz frequency; 1 mT modulation amplitude; 2 mW power) and 293 K (bottom: 9.838 GHz frequency; 0.2 mT modulation amplitude; 0.2 mW power). Right: Computed spin density plot for **4-Mn**. See Supporting Information for further details.

For **4-Mn** at 4.2 K, we observe a broad isotropic signal, line width ~2.5 mT centered at $g_{iso} = 2.004(5)$. By contrast, at room temperature the solution spectra of **4-Mn** display a rich hyperfine structure (Figure 2). These spectra are dominated by the coupling of the $^{55}$Mn nuclei ($I = 5/2$, 100%) to the electronic spin. Furthermore, contributions from ligand nuclei that have a nonzero spin are observed as emergent superhyperfine structure. By and large the two major peaks of the solution spectra can be reproduced in simulations using a spin 1/2 coupled to a single $I = 5/2$ $^{55}$Mn nucleus with a hyperfine coupling constant $a_{iso} = 1.87(5)$ mT and line width > 1 mT. On the basis of our DFT results (*vide infra*) and in agreement with the analysis of the EPR solution spectra of [(PNP)NiCl]OTf,[25] we ascribe the large line width as the result of a partially resolved hyperfine coupling to the $^{14}$N ($I = 1$, 99.63%) nucleus with $a_{iso} = 0.9$ mT. Other contributions to the hyperfine structure are expected from either one or all phosphorus atoms and aryl protons. However, from the current spectra, we are unable to delineate and assign these contributions.

At 4.2 K, **4-Re** exhibits a signal centered at $g = 2.013(1)$ that has a pseudorhombic shape with broad, shoulder-like features at $g = 2.109(4)$ and $g = 1.940(3)$ (Figure 3). The observed rhombicity is due to an anisotropic hyperfine interaction and not to an orbital contribution to the **g** tensor. At room temperature the signal recorded for **4-Re** in liquid phase exhibits a well-resolved sextet pattern arising from interaction of the electronic spin with the $^{185,187}$Re nuclei ($I = 5/2$; $^{185}$Re 37.4%; $^{187}$Re 62.6%), although no ligand superhyperfine splitting is observed. Simulations of these solution spectra yield an isotropic hyperfine splitting constant $a_{iso} = 6.01(5)$ mT, $g_{iso} = 2.013(1)$ and a line width of about 1.6 mT. Although knowledge of $A_{iso}$ combined with simulations of the low temperature spectra should allow for the determination of the dipolar part $\boldsymbol{A}_{dip}$ of the hyperfine coupling tensor $\boldsymbol{A}$, the broadness of the signal (line width ~4.7 mT) at low

(37) Chong, D.; Laws, D. R.; Nafady, A.; Costa, P. J.; Rheingold, A. L.; Calhorda, M. J.; Geiger, W. E. *J. Am. Chem. Soc.* **2008**, *130*, 2692.
(38) Hartl, F.; Vlček, A. *Inorg. Chem.* **1996**, *35*, 1257.

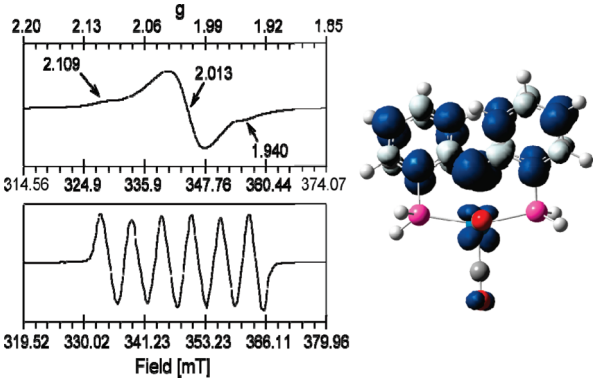


**Figure 3.** Left: EPR spectra of **4-Re** at 4.2 K (top: 9.686 GHz frequency; 1 mT modulation amplitude; 2 mW power) and 293 K (bottom: 9.838 GHz frequency; 0.2 mT modulation amplitude; 0.2 mW power). Right: Computed spin density plot for **4-Re**. See Supporting Information for further details.

temperature and the concomitant lack of resolution impedes its determination here.[39]

While the solution spectra of **4-Mn** and **4-Re** are dominated by the metal hyperfine splitting, the observed *g*-values deviate little from the free electron value $g_e = 2.0023$. Typically, low-spin $d^5$ $Re^{II}$ and $Mn^{II}$ complexes have *g*-values that are far removed from $g_e$ (i.e., $\Delta g = |g_{obs} - g_e| \geq [0.05 - 0.2]$);[40] in our case neither **4-Mn** ($\Delta g = 0.002$) nor **4-Re** ($\Delta g = 0.01$) display this behavior. Additionally, for **4-Mn** the observed metal hyperfine coupling constant (1.87 mT) is four times smaller than typical values for $Mn^{II}$ (7.5 − 10 mT).[41] While rhenium(II) complexes are rather unusual,[42,43] the reported hyperfine coupling constants for these compounds range from 32 to 84.3 mT; the value that we observe here for **4-Re** of 6.01 mT is almost 1 order of magnitude smaller than those values. The observation of well-defined spectra in room temperature solutions indicates that the spin relaxation rates are slow on the time scale of the EPR. In sum, these observations ($\Delta g \leq 0.01$, small metal hyperfine splitting constants, and well-defined EPR solution spectra at room temperature) reveal that the metal contribution to the observed EPR signals is small and the bulk of the spin density for both **4-Mn** and **4-Re** is localized on the PNP ligand. Moreover, the observation of superhyperfine structure for **4-Mn** solution spectra eliminates the possibility that the bulk of the spin density is localized on the carbonyl ligands. A similar situation to **4-Mn** is encountered for a series of *p*-phenylenediamine manganese complexes,[44] and for **4-Re** a somewhat similar ligand based radical has been described.[45]

To rationalize the ligand based oxidation event as well as the observed hyperfine splittings, we turned to computational modeling for further insight. A series of symmetrized, truncated models were constructed and geometry optimizations were performed at the B3LYP/6-311G level for manganese models and at the B3LYP/LANL2DZ level for both manganese and rhenium models. Stationary points obtained in $C_2$-symmetry closely correspond to our crystallographic data, and no geometric changes occur when all the symmetry restrictions are relieved. Analysis of the time dependent density functional theory (TD-DFT) calculations indicates that the oxidation of models representing **2-Mn** → **4-Mn** and **2-Re** → **4-Re** proceed in both cases through an electron loss from a closed shell PNP ligand orbital (see Supporting Information). Hence we find that the first coordination sphere of the metal ions is only minimally disturbed by the redox event and that only about 24%/14% (6-311G/LANL2DZ) and 7% (LANL2DZ) of the predicted spin densities are found on the metal ions in **4-Mn** and **4-Re**, respectively. In both cases we find about 50% of the spin density to be localized on the N atom while the rest is almost equally distributed over the two aryl groups (Figure 3). EPR parameters computed at the B3LYP/6-311G level predict $a_{iso} = 1.62$ mT for Mn and $a_{iso} = 0.75$ mT for N atom; these values are in good agreement with our experimental findings of 1.87(5) mT for Mn and 0.9 mT for N. We cannot estimate the Fermi contact term $a_{iso}$ for the rhenium complexes since the LANL2DZ basis replaces the lowest s orbitals with an effective potential. However, the rest of the theoretical predictions[46] conform with the structural data and the recorded EPR spectra, and taken together, indicate that along the continuum spanning the limiting resonance structures $[(PNP^{\bullet+})M^{I}(CO)_3]OTf$ ↔ $[(PNP)M^{II}(CO)_3]OTf$, compounds **4-Mn** and **4-Re** are well formulated as metal-bound diarylaminyl radical cation species, as has been observed in other metal complexes.[47−51]

**Reactivity Studies of [(PNP)M(CO)$_3$]OTf.** The ligand radical character of complexes **4-Mn** and **4-Re** implied by spectroscopy and computation is manifest in the chemical reactivity of these species. The reactivity of **4-Mn** and **4-Re** was surveyed with a suite of H-atom donors with intent of forming **3-Mn** and **3-Re**. Although neither compound reacted with triethylsilane or thiophenol, treatment with tributyltin hydride did induce reactions. The observed products of the reaction were the

(39) The shape of spectra at low temperature can be reproduced approximately using an axial *A* tensor such that $a_{\|} \approx 6.0$ mT and $a_{\perp} \approx 0$ mT. Since $a_{iso} \approx 6.0$ mT, from the solution spectra, the dipolar part of the A tensor would be such that $a_{\|\,dip} \approx \pm 12.0$ mT and $a_{\perp dip} \approx \pm 6.0$ mT. However, the current spectra lack the resolution needed for unambiguous determination of anisotropy in the hyperfine splitting.

(40) Abragam, A.; Bleaney, B. *Electron Paramagnetic Resonance of Transition Ions*; Dover: New York, 1986; Chapter 8.8.
(41) Saha, A.; Majumdar, P.; Goswami, S. *J. Chem. Soc., Dalton Trans.* **2000**, 1703.
(42) Voigt, A.; Abram, U.; Kirmse, R. *Z. Anorg. Allg. Chem.* **1999**, *625*, 1658.
(43) Sengupta, S.; Chakraborty, I.; Chakravorty, A. *Eur. J. Inorg. Chem.* **2003**, 1157.
(44) Gross, R.; Kaim, W. *Inorg. Chem.* **1987**, *26*, 3596.
(45) Abakumov, G. A.; Poddel'sky, A. I.; Bubnov, M. P.; Fukin, G. K.; Abakumova, L. G.; Ikorskii, V. N.; Cherkasov, V. K. *Inorg. Chim. Acta* **2005**, *358*, 3829.

(46) The models chosen omit alkyl substituents on the ligand phosphines and arenes for computational expediency. We have also performed calculations on the full structures of **4-Mn** and **4-Re**. We note that inclusion of substituent alkyl moieties results in only minor quantitative changes in computed values. Complete details can be found in the Supporting Information.

(47) Penkert, F. N.; Weyhermuller, T.; Bill, E.; Hildebrandt, P.; Lecomte, S.; Wieghardt, K. *J. Am. Chem. Soc.* **2000**, *122*, 9663.
(48) Buttner, T.; Geier, J.; Frison, G.; Harmer, J.; Calle, C.; Schweiger, A.; Schonberg, H.; Grutzmacher, H. *Science* **2005**, *307*, 235.
(49) Maire, P.; Konigsmann, M.; Sreekanth, A.; Harmer, J.; Schweiger, A.; Grutzmacher, H. *J. Am. Chem. Soc.* **2006**, *128*, 6578.
(50) Ingleson, M. J.; Pink, M.; Huffman, J. C.; Fan, H.; Caulton, K. G. *Organometallics* **2006**, *25*, 1112.
(51) Miyazato, Y.; Wada, T.; Muckerman, J. T.; Fujita, E.; Tanaka, K. *Angew. Chem., Int. Ed.* **2007**, *46*, 5728.

**Scheme 3.** Allylation of [(PNP)M(CO)$_3$]OTf

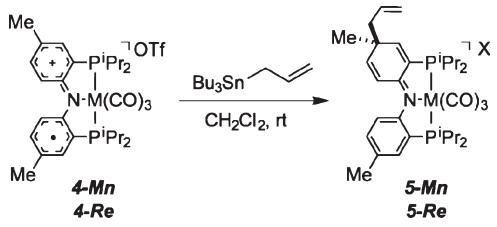


corresponding neutral pincer complexes **2-Mn** and **2-Re**, respectively. Speculating that **3-Mn** and **3-Re** initially formed and subsequently reacted with $Bu_3SnH$ via protonolysis, we sought a radical transfer reagent that would furnish a product that was robust under the reaction conditions. To this end, treatment of **4-Mn** and **4-Re** with allyl tri-*n*-butylstannane led to consumption of starting material over several hours (Scheme 3). $^1$H NMR analysis of the diamagnetic reaction products **5-Mn** and **5-Re** indicated incorporation of the allyl unit and suggested a desymmetrization of the previously homotopic arene units. Consistent with a decreased degree of symmetry, the $^{31}P\{^1H\}$ NMR spectra indicated the presence of two nonequivalent phosphorus nuclei, which we confirm by X-ray analysis (Figure 1). Allylation of the organic fragment occurs *para* relative to the amine substituent, resulting in a dearomatized iminoquinoid-type motif in the carbocyclic moiety.

## Discussion

The one-electron redox chemistry of the pincer complexes **2-Mn** and **2-Re** described here is dominated by ligand localized events. Infrared spectroscopy of the cationic complexes **3-Mn** and **3-Re** show an about 35 cm$^{-1}$ hypsochromic shift in CO stretching frequency compared to their neutral congeners. This change is not consistent with an oxidation that significantly alters metal d-electron count (and consequently M-CO $\pi$ backbonding),[52] but instead agrees well with previously reported values obtained for ligand oxidation of metal carbonyl complexes.[38,53] Recent studies have emphasized the importance of electrostatic effects on carbonyl stretching frequencies in cationic complexes,[54] and it is likely that this is responsible for the changes we observe. Specifically, introduction of unit charge to the complex by way of ligand protonation induces a shift in CO frequencies similar to that observed by one-electron oxidation. Additionally, the observation that the metal and ligand behave as distinct redox moieties in these complexes offers certain perspectives on reactivity. The ability to independently address the ligand moiety in an oxidation event likely arises from the well-resolved positions of the metal and ligand redox couples. In an alternative scenario, one would expect the metal ion to participate more cooperatively in redox chemistry as the potentials of the ligand and metal redox couples near parity. A fuller accounting of this effect by systematic modulation of the ligand subsituents and metal ions would be instructive.

In summary, PNP complexes of manganese and rhenium tricarbonyl compounds **2-Mn** and **2-Re** exhibit reversible electrochemical oxidation events at low potentials. Stoichiometric chemical oxidation results in the formation of persistent paramagnetic complexes **4-Mn** and **4-Re**. Oxidation only minimally perturbs the structure of the primary coordination sphere, and EPR spectroscopy indicates that the oxidation event is largely ligand localized. The chemical reactivity of **4-Mn** and **4-Re** is consistent with their description as metal-bound diarylaminyl radical cations. With respect to the effect of ligand oxidation on the metal, formation of a hole equivalent on the ligand results in a shift in the stretching frequencies of the carbonyl ligands of ~35 cm$^{-1}$ toward higher energy. Not only is the magnitude of this shift inconsistent with an oxidation that significantly alters metal electron count, but we note that introduction of a positive charge on the ligand by way protonation induces a similar effect.

## Experimental Section

**Materials and Methods.** All manipulations were carried out in oven-dried glassware under an inert atmosphere provided either by a $N_2$-filled glovebox or by using standard Schlenk techniques. All reaction solvents were reagent grade (Aldrich) or better and were dried and degassed by standard methods.[55] Ligands (PNP)Li **1-Li** and (PNP)H **1-H** were prepared according to the literature method.[56] $Mn(CO)_5Br$, $Re(CO)_5Br$, and AgOTf were purchased from Strem Chemical and used without further purification. $CDCl_3$ and $C_6D_6$ were purchased from Cambridge Isotope Laboratories and stored over activated 4 Å molecular sieves in the glovebox prior to use. $^1$H, $^{13}$C, and $^{31}$P NMR spectra were acquired on a Bruker DRX 400 MHz spectrometer in the specified solvent in sealable J. Young NMR tubes. $^1$H and $^{13}$C NMR spectra were calibrated against the residual protio-solvent resonances (chloroform 7.26 ppm; benzene 7.16); $^{31}$P NMR spectra were referenced externally to $H_3PO_4$ (0 ppm). EPR spectra were recorded using a Bruker EMX spectrometer outfitted with 13" magnets, an ER 4102ST cavity, and a Gunn diode microwave source producing X-band radiation. The simulations of the EPR spectra were performed using the Spincount software developed by Dr. Mike Hendrich at Carnegie Mellon University (http://www.chem.cmu.edu/groups/hendrich/facilities/index.html). Infrared spectra were acquired on a Perkin-Elmer Model 2000 FT-IR spectrophotometer in a potassium bromide matrix or in benzene solution as noted. All electrochemistry was conducted in a Vacuum Atmospheres glovebox under nitrogen, using a CHI730C potentiostat interfaced to a personal computer running CV50W software. Glassy carbon ($d$ = 3 mm) and platinum ($d$ = 2 mm) working electrodes, as well as platinum wire auxiliary electrodes, were obtained from Bioanalytical Systems. The reference electrode employed was Ag/AgCl wire in a glass frit; however, all potentials are reported relative to the $FeCp_2^{o/+}$ couple determined by addition of $FeCp_2$ to the electrochemical cell at the end of the experiment. High resolution electrospray ionization mass spectrometry was performed in the MIT Department of Chemistry Instrument Facility. Elemental analyses were performed by CALI, Inc. (Parsippany, NJ).

**Preparation of (PNP)Mn(CO)$_3$ (2-Mn). Method 1.** In a 200 mL Schlenk flask equipped with a magnetic stirbar, $Mn(CO)_5Br$ (550 mg, 2.0 mmol) was dissolved in 50 mL of dry dioxane. To this yellow-orange solution, (PNP)Li (**1-Li**) (870 mg, 2.0 mmol) was added via syringe as a solution in 50 mL of dry dioxane. The resulting mixture was heated to 100 °C

(52) Nakamoto, K. *Infrared and Raman Spectra of Inorganic and Coordination Compounds*, 6th ed.; John Wiley: Hoboken, NJ, 2009; p 132.
(53) Hartl, F.; Vlček, A. *Inorg. Chem.* **1992**, *31*, 2869.
(54) Goldman, A. S.; Krogh-Jespersen, K. *J. Am. Chem. Soc.* **1996**, *118*, 12159.
(55) Armarego, W. L. F.; Perrin, D. D. *Purification of Laboratory Chemicals*, 4th ed.; Butterworth-Heinemann: Oxford, 1996.
(56) Ozerov, O. V.; Guo, C.; Fan, L.; Foxman, B. M. *Organometallics* **2004**, *23*, 5573.

under nitrogen atmosphere for 18 h. The resulting solution was concentrated in vacuo to a red-orange residue, which was taken up in 20 mL of methylene chloride and stirred vigorously for 15 min. The resulting heterogeneous mixture was filtered to remove an off-white precipitate, and the filtrate was concentrated to about 5 mL, at which point red-orange precipitate began to form. Pentane (20 mL) was added, and the mixture stored at −10 °C for 2 d. The red-orange product was collected on a glass frit, washed with a small portion of cold pentane, and dried in vacuo. Yield of **2-Mn**: 473 mg, 42%. Crystalline material suitable for X-ray diffraction was prepared by slow evaporation of a $CH_2Cl_2$:pentane solution (2 mL, 10:1 v/v) of **2** (ca. 15 mg) at −10 °C over the course of 4 days.

**Method 2.** A 50 mL Schlenk flask was charged with **1-H** (1.2 g, 2.79 mmol), and 10 mL of hexamethyldisiloxane. $Mn_2(CO)_{10}$ (0.544 g, 1.39 mmol) was added, and the mixture was refluxed for 13 h under argon with an open condenser. During this time an orange solid was formed. The solvent was removed in vacuo, then the orange solid was dissolved in THF and filtered through silica. Removal of THF in vacuo and recrystallization from THF/pentane gave **2-Mn** as a pure microcrystalline orange solid (1.25 g, 80%). Single crystals were obtained from a concentrated $C_6D_6$ solution at room temperature. $^1$H NMR ($C_6D_6$, 400 MHz): 7.45 (dd, $J$ = 8, 3 Hz, 2H), 6.84 (d, $J$ = 4 Hz, 2H), 6.76 (d, $J$ = 8 Hz, 2H), 2.32 (m, 4H), 2.16 (s, 6H), 1.13 (m, 24 H) ppm; $^1$H NMR ($CD_2Cl_2$): 7.08 (d, $J$ = 8 Hz, 2H), 6.90 (br s, 2H), 6.74 (d, $J$ = 8 Hz, 2H), 2.60 (m, 4H), 2.19 (s, 6H), 1.24 (m, 12H), 1.19 (m, 12H) ppm; $^{31}$P{$^1$H} NMR ($C_6D_6$, 161.97 MHz) 84.1 ppm; $^{31}$P{$^1$H} NMR ($CD_2Cl_2$): 84.0 ppm; IR (KBr pellet) $\nu_{CO}$ 2020 (m), 1917 (s), 1896 (s) cm$^{-1}$; IR ($C_6D_6$) $\nu_{CO}$ 2017 (m), 1926 (s), 1893 (s) cm$^{-1}$. HRMS (ESI) Calcd for $C_{29}H_{40}MnNO_3P_2$: 567.1864, Found: 567.1869. Elem. Anal. Found (Calcd) for $C_{29}H_{40}NO_3P_2Mn$: C, 61.37 (61.46); H, 7.10 (7.26); N, 2.47 (2.60) %.

**Preparation of PNPMn(CO)$_2$. Method 1.** A 50 mL Schlenk flask was charged with PNPMn(CO)$_3$ (260 mg, 0.466 mmol) and 3 mL of mesitylene. The solution was refluxed for 6 h. During this time the orange solution turned dark blue. The solvent was removed in vacuo, then the dark blue solid was dissolved in toluene and filtered through silica. Removal of the solvent and recrystallization from toluene/pentane gave a mixture PNPMn(CO)$_2$/PNPMn(CO)$_3$ (40/60%). Longer refluxing time resulted in decomposition.

**Method 2.** To a solution of PNPMn(CO)$_3$ (60 mg, 0.323 mmol) in 1 mL of fluorobenzene was added [(*p*-cymene)RuCl$_2$]$_2$ (55 mg, 0.178 mmol). The solution was stirred at 60 °C for 3 days. All volatiles were removed in vacuo. The resulting residue was dissolved in $C_6D_6$ and filtered through silica. $^1$H NMR showed a mixture PNPMn(CO)$_2$/PNPMn(CO)$_3$ (73/27%). $^1$H NMR ($C_6D_6$): $\delta$ 7.41 (d, $J$ = 8 Hz, 2H), 6.89 (d, $J$ = 8 Hz, 2H), 6.72 (d, $J$ = 8 Hz, 2H), 2.55 (m, 4H), 2.10 (s, 6H), 1.27 (m, 12H), 1.08 (m, 12H) ppm; $^{31}$P{$^1$H} NMR ($C_6D_6$): $\delta$ 83.0 ppm; IR ($C_6D_6$) $\nu_{CO}$ 1900 (s), 1838 (s) cm$^{-1}$.

**Preparation of [(PN(H)P)Mn(CO)$_3$][OTf] (3-Mn).** A 25 mL Schlenk flask was charged with **2-Mn** (100 mg, 0.179 mmol) and 10 mL of toluene. Triflic acid (16 $\mu$L, 0.179 mmol) was added via syringe at which time the solution turned immediately from orange to light green. The mixture was stirred for an additional 20 min. Removal of the solvent in vacuo and recrystallization from THF/pentane gave a pure light green solid (118 mg, 92%). Single crystals of **3-Mn** were formed by diffusion of pentane into a concentrated THF solution at −35 °C. $^1$H NMR ($C_6D_6$) 9.55 (br s, 1H), 7.44 (d, $J$ = 8 Hz, 2H), 6.91 (s, 2H), 6.83 (d, $J$ = 8 Hz, 2H), 2.93 (m, 2H), 2.35 (m, 2H), 2.01 (s, 6H), 1.16 (m, 18H), 0.95 (m, 6H) ppm; $^1$H{$^{31}$P}($CD_2Cl_2$): 8.34 (s, 1H), 7.36 (s, 2H), 7.26 (d, 2H, $J$ = 8 Hz), 7.24 (d, 2H, $J$ = 8 Hz), 3.02 (m, 4H), 2.43 (s, 6H), 1.51 (d, 6H, $J$ = 7 Hz), 1.41 (d, 6H, $J$ = 7 Hz), 1.31 (d, 6H, $J$ = 8 Hz), 1.27 (d, 6H, $J$ = 8 Hz) ppm; $^{19}$F NMR ($C_6D_6$): −80.5 ppm; $^{31}$P{$^1$H} NMR ($C_6D_6$): 78.2 ppm; IR $\nu_{CO}$ (KBr pellet) 2039 (m), 1949 (s), 1923 (s) cm$^{-1}$. IR $\nu_{CO}$ ($C_6D_6$) 1953 (m), 1923 (s), 1894 (s) cm$^{-1}$. Elem. Anal. Found (Calcd) for $C_{29}H_{40}NO_3P_2Mn$: C, 50.28 (50.21); H, 5.96 (5.76) %.

**Preparation of [(PNP)Mn(CO)$_3$]OTf (4-Mn).** In a 50 mL round-bottom flask with a magnetic stirbar, ($^i$Pr$_2$PNP)Mn(CO)$_3$ (**2-Mn**) (400 mg, 0.70 mmol) was dissolved in 10 mL of $CH_2Cl_2$. A solution of AgOTf (181 mg, 0.70 mmol) in 15 mL of $CH_2Cl_2$ was then added dropwise via pipet, at which time the reaction mixture became blue. The resulting mixture was stirred at ambient temperature for 1 h, then the reaction mixture was filtered over a glass frit. The precipitate was washed with methylene chloride (2 × 15 mL) until the washings were colorless and a gray precipitate remained on the frit. The dark blue filtrate was concentrated to a residue, redissolved in methylene chloride (5 mL) then treated with pentane (15 mL) to induce precipitation of the product as a dark blue powder, which was collected and washed with pentane. Yield of **3**: 490 mg, 98%. Crystals of **4-Mn·CH$_2$Cl$_2$** suitable for X-ray diffraction analysis were prepared by vapor diffusion of pentane into a methylene chloride solution of **4-Mn** at −10 °C over the course of 3 days. IR $\nu_{CO}$ (KBr pellet) 2032 (m), 1951 (s), 1938 (s) cm$^{-1}$. HRMS (ESI) Calcd for $[C_{29}H_{40}MnNO_3P_2]^+$: 567.1864, Found: 567.1873.

**Preparation of [(allyl-PNP)Mn(CO)$_3$][Bu$_3$Sn(OTf)$_2$] (5-Mn).** In a 20 mL scintillation vial with a magnetic stirbar, [($^i$Pr$_2$PNP)Mn(CO)$_3$]OTf (**4-Mn**) (72 mg, 1.0 mmol) was dissolved in 5 mL of methylene chloride. Allyl tributylstannane (62 $\mu$L, 2.0 mmol) was added via syringe, and the reaction mixture was stirred at ambient temperature overnight. During this time the blue reaction mixture became orange and a dark precipitate formed. The crude mixture was filtered, and the filtrate was concentrated to about 0.5 mL. Pentane (ca. 5 mL) was gently layered on top, and the mixture was cooled to −10 °C overnight. The resulting orange solid was collected, washed with a 5 mL portion of pentane, and dried in vacuo. Yield of **5-Mn**: 71 mg (60%) Crystals suitable for X-ray diffraction were prepared by diffusion of pentane into a methylene chloride solution of **5-Mn** (ca. 10 mg in 1 mL) at −10 °C over the course of 4 days, resulting in the deposition of crystalline orange plates of [(allyl-$^i$Pr$_2$PNP)Mn(CO)$_3$]OTf. $^1$H NMR ($CDCl_3$, 400 MHz) 7.36 (d, $J$ = 6.4 Hz, 1H), 7.29 (d, $J$ = 8.0 Hz, 1H), 7.06 (m, 1H), 7.02 (m, 1H), 6.89 (m, 1H), 6.75 (d, $J$ = 9.6 Hz, 1H), 5.49 (m, 1H), 5.12−5.05 (m, 2H), 2.82 (br m, 4H), 2.53 (m, 2H), 2.47 (s, 3H), 1.72−1.27 (m, 45H), 0.87 (m, 9H) ppm; $^{31}$P{$^1$H} NMR ($CDCl_3$, 161.97 MHz) 86.5, 80.8 ppm; IR $\nu_{CO}$ (KBr pellet) 2034 (m), 1947 (s), 1929 (s) cm$^{-1}$. HRMS (ESI) Calcd for $[C_{32}H_{45}MnNO_3P_2]^+$: 608.2250, Found: 608.2240.

**Preparation of (PNP)Re(CO)$_3$ (2-Re).** In a 200 mL Schlenk flask equipped with a magnetic stirbar, Re(CO)$_5$Br (810 mg, 2.0 mmol) was dissolved in 50 mL of dry dioxane. To this yellow solution, ($^i$Pr$_2$PNP)Li (**1-Li**) (870 mg, 2.0 mmol) was added via syringe as a solution in 50 mL of dry dioxane. The mixture was heated to 100 °C under nitrogen atmosphere for 18 h. The resulting solution was concentrated in vacuo to a yellow residue, which was taken up in 20 mL of methylene chloride and stirred vigorously for 15 min. The mixture was filtered to remove an off-white precipitate, and the filtrate was concentrated to about 5 mL, at which point yellow precipitate began to form. Pentane (20 mL) was added, and the mixture stored at −10 °C for 2 d. The yellow product was collected on a glass frit, washed with a small portion of cold pentane, and dried in vacuo. Yield of **2-Re**: 577 mg, 41%. Crystalline material suitable for X-ray diffraction was prepared by slow evaporation of a $CH_2Cl_2$:pentane solution (2 mL, 10:1 v/v) of **2-Re** (ca. 15 mg) at −10 °C over the course of 4 days. $^1$H NMR ($C_6D_6$, 400 MHz) 7.50 (d, $J$ = 8.8 Hz, 2H), 6.85 (s, 2H), 6.75 (d, $J$ = 8.8 Hz, 2H), 2.21 (m, 4H), 2.16 (s, 6H), 1.12−1.02 (m, 24H) ppm; $^{31}$P{$^1$H} NMR ($C_6D_6$, 161.97 MHz) 45.4 ppm; IR $\nu_{CO}$ (KBr pellet) 2026 (m), 1909 (s), 1891 (s) cm$^{-1}$. HRMS (ESI) Calcd for $C_{29}H_{40}ReNO_3P_2$: 699.2044, Found: 699.2019.

**Preparation of [(PN(H)P)Re(CO)$_3$][OTf] (3-Re).** In a screw top vial charged with magnetic stirbar, **2-Re** (58 mg, 0.080 mmol) was dissolved in 2 mL of methylene chloride. Triflic acid (0.1 mL; 1.0 M in $CH_2Cl_2$) was added via syringe, at which point the yellow solution became very faintly light blue. The mixture was stirred for 15 min, then diluted with pentane (5 mL) and placed in a −40 °C freezer. Slow evaporation yielded colorless crystals of **3-Re** suitable for crystallography. $^1$H NMR ($C_6D_6$): 10.48 (s, 1H), 7.46 (d, $J$ = 6.8 Hz, 2H), 6.87 (s, 2H), 6.79 (d, $J$ = 8.0 Hz, 2H), 2.86 (m, 2H), 2.22 (m, 2H), 2.00 (s, 6H), 1.07 (m, 18H), 0.82 (m, 6H) ppm; $^{31}$P{$^1$H} NMR ($C_6D_6$): $\delta$ 42.3 ppm; $\nu_{CO}$ (KBr pellet) 2048 (m), 1943 (s), 1929 (s) cm$^{-1}$.

**Preparation of [(PNP)Re(CO)$_3$]OTf (4-Re).** In a 50 mL round-bottom flask with a magnetic stirbar, ($^i$Pr$_2$PNP)Re(CO)$_3$ (**2-Re**) (800 mg, 1.14 mmol) was dissolved in 10 mL of $CH_2Cl_2$. A solution of AgOTf (294 mg, 1.14 mmol) in 15 mL of $CH_2Cl_2$ was then added dropwise via pipet, at which time the reaction mixture became blue. The resulting mixture was stirred at ambient temperature for 1 h, then filtered over a glass frit. The precipitate was washed with methylene chloride (2 × 15 mL) until the washings were colorless and a gray precipitate remained on the frit. The blue filtrate was concentrated to a residue, redissolved in methylene chloride (5 mL) then treated with pentane (15 mL) to induce precipitation of the product as a royal blue powder, which was collected and washed with pentane. Yield of **4-Re**: 883 mg, 86%. Crystals of **4-Re·CH$_2$Cl$_2$** suitable for X-ray crystallography were prepared by vapor diffusion of pentane into a methylene chloride solution of **4-Re** at −10 °C over the course of 3 days. IR $\nu_{CO}$ (KBr pellet) 2054 (m), 1951 (s), 1934 (s) cm$^{-1}$. HRMS (ESI) Calcd for $[C_{29}H_{40}ReNO_3P_2]^+$: 699.2044, Found: 699.2064.

**Preparation of [(allyl-PNP)Re(CO)$_3$][Bu$_3$Sn(OTf)$_2$] (5-Re).** In a 20 mL scintillation vial with a magnetic stirbar, [($^i$Pr$_2$PNP)Re(CO)$_3$]OTf (**4-Re**) (85 mg, 1.0 mmol) was dissolved in 5 mL of methylene chloride. Allyl tributylstannane (62 $\mu$L, 2.0 mmol) was added via syringe, and the reaction mixture was stirred at ambient temperature for 2 h. During this time the blue reaction mixture became yellow and a dark precipitate formed. The crude mixture was filtered, and the filtrate was concentrated to about 0.5 mL. Pentane (ca. 5 mL) was gently layered on top, and the mixture was cooled to −10 °C overnight. The resulting dark yellow solid was collected, washed with a 5 mL portion of pentane, and dried in vacuo. Yield of **5-Re**: 56 mg (41%). Crystals suitable for X-ray diffraction were prepared by diffusion of pentane into a methylene chloride solution of **5-Re** (ca. 10 mg in 1 mL) at −10 °C over the course of 4 days, resulting in the deposition of crystalline yellow plates. $^1$H NMR ($CDCl_3$, 400 MHz) 7.37 (d, $J$ = 6.4 Hz, 1H), 7.31 (d, $J$ = 8.4 Hz, 1H), 7.13 (m, 1H), 7.01 (d, $J$ = 8.4 Hz, 1H), 6.97 (m, 1H), 6.81 (d, $J$ = 10.4 Hz, 1H), 5.48 (m, 1H), 5.11 (d, $J$ = 17.4 Hz, 1H), 5.06 (d, $J$ = 10.4 Hz, 1H), 2.79 (br m, 4H), 2.55 (m, 2H), 2.51 (s, 3H), 1.73−1.14 (br m, 45H), 0.87 (m, 9H) ppm; $^{31}$P{$^1$H} NMR ($CDCl_3$, 161.97 MHz) $\delta$ 47.1 (d, $J$ = 102 Hz, 1P), 44.6 (d, $J$ = 102 Hz, 1P) ppm; IR $\nu_{CO}$ (KBr pellet) 2046 (m), 1946 (s), 1928 (s) cm$^{-1}$. HRMS (ESI) Calcd for $[C_{32}H_{45}ReNO_3P_2]^+$: 740.2436, Found: 740.2422.

**Acknowledgment.** Research was supported by the National Science Foundation, Center for Chemical Innovation CHE-0533150 (D.G.N. and O.V.O) and by NSF CHE-0517798 and CHE-0809522 the Petroleum Research Fund, the Sloan Foundation, and the Dreyfus Foundation (O.V.O.). We also thank the National Science Foundation for the partial support of this work through Grant CHE-0521047 for the purchase of a new X-ray diffractometer at Brandeis University. A.T.R. and J.G.M. acknowledge the NIH for NRSA postdoctoral fellowships.

**Supporting Information Available:** Synthetic procedures, spectral and crystallographic data, and computational details. This material is available free of charge via the Internet at http://pubs.acs.org.